

## Use of activated carbon from NiO modified Polyethylene Terephthalate Plastic bottle waste to optimize natural gas storage in Adsorbed Natural Gas (ANG) technology



Yuliusman Yuliusman<sup>1</sup>, Athaya Khanza Kamilia<sup>1</sup>, Anggi Nugroho Utomo<sup>1</sup>, Nasruddin Nasruddin<sup>2</sup>

<sup>1</sup>Department of Chemical Engineering, Faculty of Engineering, Universitas Indonesia, Indonesia

<sup>2</sup>Department of Mechanical Engineering, Faculty of Engineering, Universitas Indonesia, Indonesia

### Abstract

Storage and transportation of natural gas are major challenges in optimizing energy use. To overcome the challenges, Adsorbed Natural Gas (ANG) technology offers a promising alternative for increasing storage capacity at lower pressures. Therefore, this study aims to explore the efficiency of waste polyethylene terephthalate (PET) bottle converted into activated carbon through pre-treatment, carbonization, chemical activation with 4 M KOH, and physical activation using  $N_2$  flow. Modification of activated carbon was carried out using NiO metal impregnation at concentrations of 0.5%, 1%, and 2% to enhance adsorption performance. The results of characterization using iodine number, scanning electron microscopy (SEM), and energy dispersive X-ray spectroscopy (EDS) showed that the 2% NiO-impregnated sample had the highest surface area of  $997.65\text{ m}^2/\text{g}$ . Natural gas adsorption and desorption testing showed that this material achieved the maximum storage capacity of 138.9 g/kg at  $28^\circ\text{C}$  and 9 bar, with superior performance compared to non-impregnated samples and several previously reported ANG adsorbent. These results showed that combining NiO modification with KOH-activated PET waste improved methane uptake beyond commercial activated carbons and provided an environmentally sustainable solution for plastic waste valorization.

### Keywords:

Absorbed Natural Gas (ANG);  
Activated Carbon;  
NiO;  
Polyethylene Terephthalene (PET) Bottles Waste;

### Article History:

Received: May 29, 2025

Revised: September 16, 2025

Accepted: October 3, 2025

Published: January 8, 2026

### Corresponding Author:

Yuliusman Yuliusman  
Department of Chemical Engineering, Faculty of Engineering, Universitas Indonesia, Indonesia  
Email: [usman@che.ui.ac.id](mailto:usman@che.ui.ac.id)

This is an open access article under the [CC BY-SA license](https://creativecommons.org/licenses/by-sa/4.0/)



### INTRODUCTION

Energy demand in Indonesia is continuously increasing along with population growth and economic development. In response to this increase, the government has set a target to raise natural gas usage to 22% of the national energy mix by 2025, equivalent to 8300 MMSCFD [1][2]. However, natural gas storage and transportation remain challenging due to the low density and the need for high-pressure storage tanks.

To address the challenges, Adsorbed Natural Gas (ANG) technology has become a promising alternative, enabling natural gas storage at near-ambient temperature and lower

pressure compared to Compressed Natural Gas (CNG). This technology also maintains comparable capacity [3], with the efficiency significantly dependent on adsorbent properties. Activated carbon is the most widely used adsorbent due to the large surface area, microporous structure, and high adsorption capacity [4][5].

Activated carbon is conventionally produced from precursors such as coal, coconut shells, or wood [6]. However, these sources do not address the increasing problem of plastic waste. For example, Indonesia generates 3.22 million metric tons of plastic waste annually, ranking second globally in

ocean plastic disposal [7]. Among various types of plastic, polyethylene terephthalate (PET) is a promising alternative precursor for producing activated carbon. PET contains approximately 60% carbon and offers a valuable pathway for addressing plastic pollution.

Several studies have shown that chemical activation with potassium hydroxide (KOH) and physical activation with inert gases can develop well-structured microporosity [8][9]. Beyond precursor and activation methods, metal impregnation has been reported to further enhance gas adsorption performance. For instance, NiO modification has been shown to increase methane adsorption and desorption capacity due to the development of additional active sites and improved interaction with  $\text{CH}_4$  molecules [10]. Compared to other metals such as Zn or Mg, NiO has superior catalytic and adsorption-enhancing properties, serving as a strong candidate for ANG applications.

Based on the description, this study was conducted on the production of activated carbon using PET raw material, which was carbonized, chemically activated with KOH, and physically activated with  $\text{N}_2$  gas. An application impregnated with a  $(\text{Ni}(\text{NO}_3)_2 \cdot 6\text{H}_2\text{O})$  metal solution was used to enhance the surface area of activated carbon, thereby improving performance. KOH was used as an active substance to produce activated carbon with favorable moisture and ash content, iodine number, and surface area. The activated carbon was then tested as an adsorbent for adsorption and desorption performance in ANG tanks under varying pressures and temperatures. This study's novelty lies in using PET plastic waste as a precursor combined with NiO impregnation, which remains largely unexplored for ANG storage applications. This method addresses plastic waste management and provides a sustainable pathway to develop high-performance adsorbent for clean energy storage [11].

## METHOD

### Material

This study was conducted through several main processes, namely carbonization, chemical and physical activation, as well as metal impregnation. Characterization was performed using iodine number test, while surface morphology of activated carbon samples was observed using scanning electron microscopy (SEM, Zeiss). The determination of elemental components in the activated carbon sample was investigated through energy dispersive X-ray spectroscopy (EDS, Bruker). This was followed

by testing activated carbon in ANG technology to determine the storage and release capacity of natural gas.

### Methods

Activated carbon was tested for the implementation of natural gas storage in ANG technology with variations in pressure and storage temperature to obtain data on adsorption and desorption capacity of natural gas. This research was expected to make plastic waste an alternative raw material for producing activated carbon that could be used as adsorbent in natural gas storage in ANG technology.

Methane gas testing was conducted to evaluate adsorption and desorption capacity of the synthesized activated carbon for ANG technology. The sample was loaded into ANG cylinder, and the testing procedure was carried out in several stages, including degassing, void volume measurement, adsorption capacity testing, and desorption capacity testing. [Figure 1](#) presents the schematic of ANG testing apparatus used in this study [12].

The experiment started with the preparation of PET raw materials, which included washing and cutting PET plastic waste. The samples collected were subjected to carbonization to remove volatile substances at a temperature of  $480^\circ\text{C}$  for 120 minutes. This was followed by chemical activation using a 4 M KOH activator for 120 minutes at a temperature of  $80^\circ\text{C}$ . The samples were washed using HCl and physically activated with a flow of  $\text{N}_2$  gas at  $100 \text{ ml} \cdot \text{min}^{-1}$  at a temperature of  $800^\circ\text{C}$  for 120 minutes. To enhance adsorption capability, the samples were metal impregnated using NiO with varying concentrations of 0.5%, 1%, and 2% to determine the concentration with the best results.

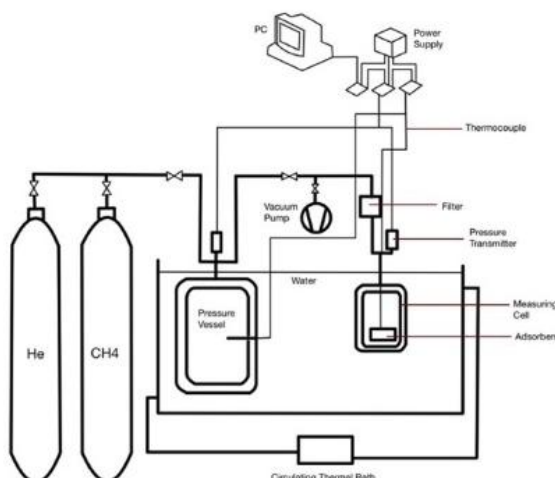


Figure 1. ANG Testing Apparatus Schematic

The final samples were characterized through iodine number tests to determine the iodine number and surface area. This was followed by characterization using SEM EDS to identify the morphological structure and content of activated carbon. The samples were tested in ANG tubes to determine adsorption and desorption capacity by varying the pressure at 3, 5, 7, and 9 bar, as well as temperature variations at 28; 31; and 35°C.

## RESULTS AND DISCUSSION

### Carbonization Results

Carbonization process serves as the initial stage in the production of activated carbon. The principle at work includes the release of volatile substances contained in the plastic, leaving behind pure carbon, which leads to the formation of pores. At temperature between 100-200°C, white smoke appears, and the smell of burning plastic can be detected, indicating that the volatile substances have evaporated at their boiling points. During this stage, the ester bonds in PET plastic polymer chain break down when heated, producing terephthalic acid (TPA) and ethylene glycol as monomers. At approximately 250°C, PET experiences thermal decomposition, producing simpler substances such as CO<sub>2</sub>, CO, water, and other byproducts. As the temperature increases, specifically to 300°C, black residue in the form of remaining carbon starts to form. Carbon content is optimally obtained at 480°C and porosity or open pores have formed. In this study, carbonization process produced an average yield of 11.53%, due to the high temperature over an extended carbonization period, leading to excessive decomposition, as shown in Table 1.

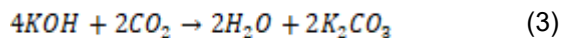
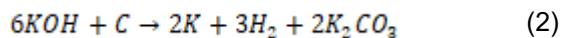
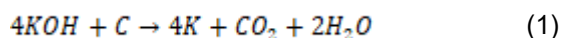
### Chemical Activation Results

The purpose of chemical activation is to decompose the molecules in carbon, forming a porous structure that can increase adsorption capacity.

Table 1. Carbonization Yield

No.	Mass Before Carbonization (g)	Mass After Carbonization (g)	Yield (%)
1.	43.42	4.24	9.58
2.	42.11	4.52	10.91
3.	44.41	4.33	9.88
4.	42.87	3.52	8.08
5.	42.65	5.20	11.99
6.	52.48	13.67	11.74
<b>Yield Average</b>			11.53

Additionally, activation has the potential to change the chemical and structural properties of the activated carbon, enhancing the efficiency of capturing and binding contaminated molecules. In this study, a chemical activator containing a metal hydroxide, specifically 4 M KOH, was used. During the stirring process, a reaction occurred between carbon and KOH activator, as shown in the following chemical equations:



Acting as a strong base, KOH can remove impurities in carbon from carbonization. KOH is adsorbed when interacts with carbon, leading to a reaction that forms an intermediate compound, potassium carbonate (K<sub>2</sub>CO<sub>3</sub>). In this context, carbonate compound plays a role in controlling the size and distribution of pores in activated carbon. Oxygen content also reacts with carbon (C), leading to partial oxidation that produces carbon dioxide. Hydrogen gas is released due to thermal decomposition reactions. From this dehydration reaction, carbon is eroded, and the surface area of activated carbon increases due to the formation of additional pores.

### Physical Activation Results

After chemical activation stage, carbon is further activated physically to expand the pores and obtain mesoporosity in the structure. In this study, physical activation was performed by heating at 800°C for 2 hours with a nitrogen gas flow of 100 ml·min<sup>-1</sup>. Nitrogen gas acted as an activating gas, reacting with carbon to open pores and increase the surface area. It also functioned as an inert gas that prevented oxygen from entering and reacting to cause combustion. Based on the results in Table 2, physical activation obtained an average of 79.93%, due to the presence of residual volatile compounds from the previous stage, which burned off at high temperatures. In this study, nickel (II) nitrate hexahydrate (Ni(NO<sub>3</sub>)<sub>2</sub>·6H<sub>2</sub>O) dissolved in distilled water was used as the impregnator.

### Metal Oxide Impregnation Results

The final step in the production of activated carbon is metal oxide impregnation, an additional treatment to enhance adsorption capabilities. Subsequently, activated carbon was impregnated in NiO solution at a ratio of 1:2 through a stirring process at 70°C for 2 hours.

Table 2. Physical Activation Yield

No.	Mass Before Physical Activation (g)	Mass After Physical Activation (g)	Yield (%)
1.	50.3	46.61	92.66
2.	60.05	46.49	77.42
3.	59.13	40.51	68.51
4.	60	48.67	81.12
Yield Average			79.93

During this stage, a decomposition reaction occurred, leading to the formation of NiO, CO<sub>2</sub>, and H<sub>2</sub>O. The activated carbon was dried in an oven at 110°C to remove moisture and volatile compounds on the carbon surface after impregnation. The heating process also played a role in the dissociation of nitrate hexahydrate into NiO [13].

### Iodine Number Results

The surface area of activated carbon was evaluated using iodine number method. The selection of this method was due to simplicity, cost-effectiveness, and the ability to provide a rapid estimation of micropore surface area, relevant to adsorption processes comprising small molecules. Iodine number had also been identified as a widely accepted quality indicator in industrial applications of activated carbon (ASTM D4607). Although BET method is recognized as a more precise and comprehensive method for determining total surface area and pore distribution, iodine number offers a practical and reliable alternative, specifically in the absence of BET facilities. Therefore, the use of iodine method provides a representative measure of adsorbent surface area and adsorption capability.

Iodine number indicates adsorption capacity of activated carbon towards iodine. In this study, iodine number test was conducted to determine the surface area and adsorption capacity of the produced activated carbon samples. The results obtained are shown in Table 3.

Based on the results, a decrease in iodine number was observed from the carbonization to the physical activation sample. This was due to the high temperature used during the physical activation process, which damaged or closed pores because of excessive heat. For the impregnated samples, the highest iodine number was obtained in 2% NiO. The modified activated carbon has an increasing iodine number due to the formation of new pores and active sites.

Table 3. Iodine Number

Sample	Iodine Number (mg/g)	Surface Area (m <sup>2</sup> /g)
Carbonization	1025.45	1019.89
Chemical activation	1025	1019.44
Physical activation	946.73	941.6
0.5% NiO	930.74	925.69
1% NiO	978.65	973.35
2% NiO	1003.09	997.65

### Scanning Electron Microscopy (SEM) Characterization

Characterization method used SEM to observe the surface structure of activated carbon samples. In this study, tests were conducted on carbonization, physical activation, and the impregnated stage samples with the highest iodine number. The result of SEM test is shown in Figures 2 and 3.

In carbonization sample, only plates containing some powder in the form of ash or impurities were visible. Physical activation showed the formation of pores due to the reaction between carbon and KOH activator with N<sub>2</sub> gas, alongside reduced impurities. SEM images of the 2% NiO-impregnated samples showed a significantly rougher and more heterogeneous surface compared to the others. This morphological change showed the formation of larger and more irregular pores, suggesting that NiO played a significant role in enhancing pores development during the activation process.

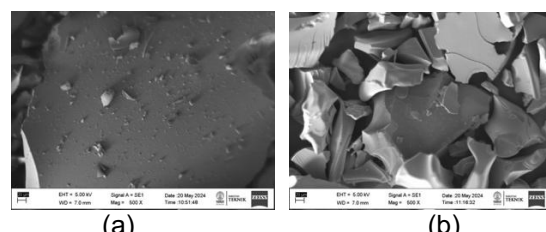


Figure 2. SEM Test Results for Physical Activation Sample at: (a) 500x Magnification and (b) 1000x Magnification

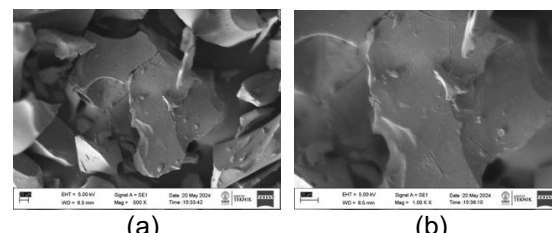


Figure 3. SEM Test Results for 2% NiO Impregnated Sample at: (a) 500x Magnification and (b) 1000x Magnification

## Energy Dispersive X-Ray Spectroscopy (EDS) Characterization

EDS testing is a characterization method used to determine the elemental components in activated carbon sample. In this study, testing was conducted on three samples, including carbonization, physical activation, and impregnation with the best iodine number. Table 4 shows EDS test results containing the components in each sample.

In carbonization stage, carbon content was observed to be very high at 88.77%. This indicated the formation of carbon and degradation of residues from PET due to the carbonization treatment. Subsequently, in the stage after physical activation, there was a significant decrease in oxygen content in the activated carbon, due to the high-temperature treatment causing a reduction in the percentage of oxygen.

Impregnation with 2% NiO metal showed that carbon content decreased from 87.91% to 73.86%. This decrease was attributed to the impregnation of Ni, which had a larger molecular weight compared to carbon. The increase in oxygen atoms was due to the oxygen from Ni impregnation bonding with active sites on activated carbon.  $(Ni(NO_3)_2 \cdot 6H_2O)$  is capable of creating new pores, which also contributes to this effect. The presence of Pt in EDX results is due to the use of a platinum conductor required for sample analysis.

## Void Volume Results

Void volume testing can characterize the porosity and volume of activated carbon. In this stage, an inert gas, helium, was used due to the non-reactive nature with activated carbon, ensuring no chemical or structural changes. The calculation of void volume was performed by measuring the moles of helium entering the filling and adsorption tank. The two types of samples tested were KNI and KI for physical activation and impregnation, respectively, with void volume values as shown in Table 5.

Table 4. EDS Characterization Results

Element	Carbonization Sample (%)	Physical Activation Sample (%wt)	NiO 2% Impregnation Sample (%wt)
C	88.77	87.91	73.86
O	6.29	0.51	15.19
Pt	4.95	11.58	6.14
Ni	-	-	4.82

Table 5. Void Volume

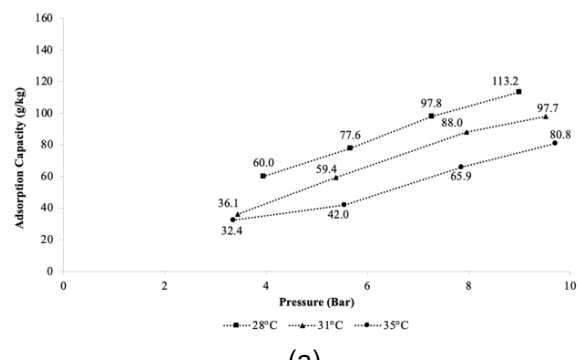
Sample	Void Volume (cm <sup>3</sup> )
KNI	319.27
KI	329.35

Based on the results, void volume value in KI sample was higher compared to KNI. This indicated that KI sample had a larger volume or space capable of accommodating adsorbed natural gas. The higher volume was due to the formation of more or wider pores after the impregnation process.

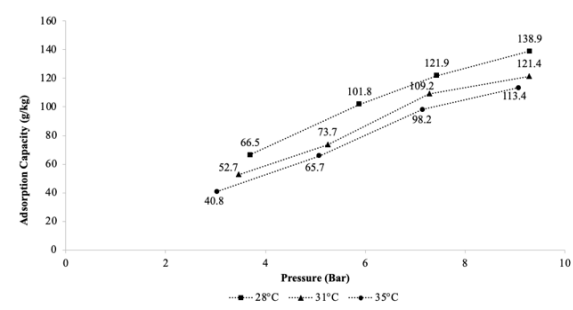
## Natural Gas Adsorption Results

Natural gas adsorption capacity is the main stage in the series of tests. In this stage, a sample of 2.5 grams was used with methane gas as adsorbate. The variations conducted were temperature (28°C, 31°C, and 35°C) as well as pressure (3, 5, 7, and 9 bar). This testing was performed isothermally by maintaining temperature with varying pressure. Figure 4 shows the graph obtained from adsorption capacity calculations.

The graph shows an increase in adsorption capacity with rising pressure. This suggests that adsorption pressure increases alongside density of natural gas, which enhances the interaction between the natural gas and the activated carbon [14].



(a)



(b)

Figure 4. Adsorption Results for:  
(a) KNI and (b) KI

With higher pressure, natural gas is also pushed into pores of the activated carbon, allowing for greater absorption. However, the effect of temperature on adsorption capacity shows a different pattern, where lower values produce a higher quantity of adsorbate per unit mass of adsorbent. This process is exothermic, indicating that at lower temperature, natural gas has reduced kinetic energy, enhancing attraction to pores of the activated carbon. Additionally, a difference in the highest adsorption capacity can be observed between the KNI and KI samples, with an increase of 22.68%.

Figure 5 shows adsorption isotherms of non-modified and Ni-modified samples at 28°C, 31°C, and 35°C. Error bars, represented by the standard deviation for each condition, are included to show the variability in the experimental data. Furthermore, the isotherms show the relationship between adsorption capacity ( $q$ ) and equilibrium pressure ( $C_e$ ), allowing a clear comparison of the effect of Ni modification and temperature on adsorption behavior.

As shown in Figure 5, Ni-modified samples consistently had higher adsorption capacities than the non-modified samples across all pressure and temperature. At 28°C and 9 bar, Ni-modified adsorbent reached  $\sim 135$  g·kg $^{-1}$  compared to  $\sim 115$  g·kg $^{-1}$  for the non-modified sample. The enhancement persisted at higher temperature, although the overall adsorption capacity decreased at 31°C and 35°C, and the performance gap narrowed. This was characteristic of the exothermic nature of physical adsorption, confirming that Ni modification significantly improved adsorption efficiency, particularly under lower thermal conditions.

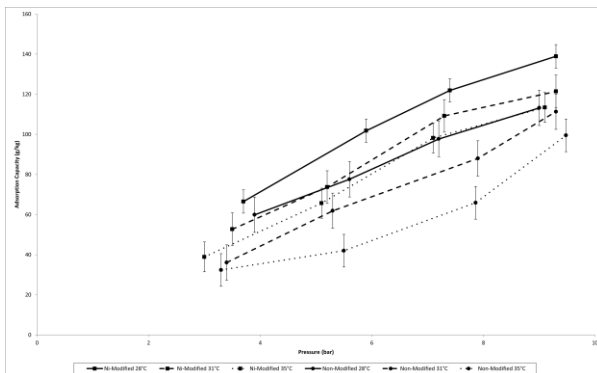


Figure 5. Adsorption isotherms of non-modified and Ni-modified samples at different temperatures with error bars

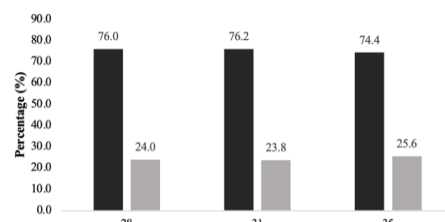
## Natural Gas Desorption Results

Natural gas desorption capacity test was conducted as a performance parameter for activated carbon. Desorption capacity value was generally lower than the storage capacity because some natural gas was trapped in the activated carbon. In this study, desorption capacity was calculated by measuring the amount of gas released when the pressure was reduced from 9 bar to 1 bar using a Coriolis flow meter. Figure 6 shows the percentage of the sample that desorbed and remained in activated carbon based on adsorption value.

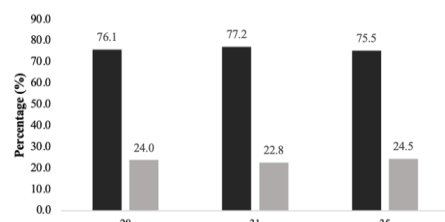
The amount of residual natural gas indicates that active sites are reduced due to incomplete desorption. Specifically, Van der Waals forces occur between natural gas and activated carbon surface.

The isothermal desorption process is considered inefficient because the system struggles to absorb heat [15]. Additionally, a higher operating temperature of the system leads to better desorption capability. This is because desorption is endothermic, and higher temperatures provide the energy needed to break the bonds between natural gas molecules and adsorbent surface.

After obtaining desorption capacity data, the efficiency of desorption process can be calculated. This is conducted by dividing the amount of natural gas desorbed at 1 bar pressure by the cumulative amount of gas adsorbed at 9 bar pressure.



(a)



(b)

Figure 6. Desorption Percentage of:  
(a) KNI and (b) KI

Based on the graph in Figure 7, the results for KI sample are superior to KNI, which is also shown by the larger surface area and void volume.

When natural gas is desorbed, heat is absorbed, leading to a decrease in system temperature, which shifts the equilibrium to the right and reduces the release of gas molecules. Therefore, desorption process requires heat for improvement as the system temperature increases [15]. In Figure 8, a decrease in desorption efficiency is observed for both samples tested at 35°C. This is due to changes in the structure of activated carbon used or increased ion movement at high temperatures, causing difficulty in the detachment of adsorbed ions. To evaluate the performance of activated carbon in this study, adsorption data were compared with previous studies.

Previous studies showed that both the selection of activator and modification method significantly influenced activated carbon performance. Olam (2022) reported low surface area using  $ZnCl_2$ , while An et al. (2023) showed that high surface area did not correlate with elevated methane uptake. Solís et al. [13] emphasized the potential of plastic waste as a precursor, although focusing on  $CO_2/CH_4$  separation.

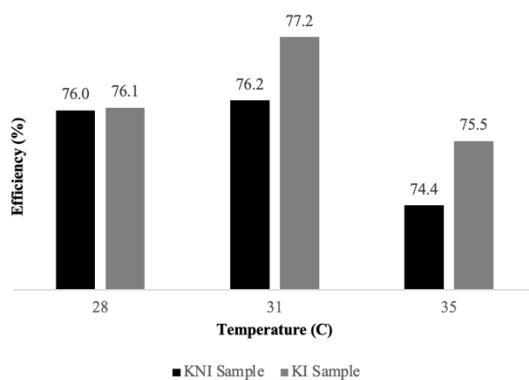


Figure 7. Efficiency of Desorption of KNI and KI

Author & Year	Raw Material & Activation	Modification	Surface Area ( $m^2/g$ )	Adsorption Capacity (g/kg)
This Study (2024)	PET, KOH activation	2% NiO	979.18	148.05
Olam (2022)	PET, $ZnCl_2$ activation	None	313.05	Not specified
An et al. (2023)	Commercial activated carbon	None	1629	~126
Solis et al. (2024)	Mixed plastic waste, KOH/ $K_2CO_3$ activation	None	~1100	Not specified (focused on $CO_2/CH_4$ selectivity)

Figure 8. Comparative Performance of Activated Carbon

In comparison, this study introduced a new method by applying NiO modification to KOH-activated PET carbon, which significantly enhanced methane in ANG technology adsorption capacity.

## CONCLUSION

In conclusion, the production of activated carbon through KOH and nitrogen gas causes a decrease in surface area based on iodine number calculations. However, activated carbon shows better pores structure, with 2% NiO impregnation achieving a surface area of 997.65  $m^2/g$ . The highest storage capacity of 138.886 g/kg with desorption efficiency of 76.05% is achieved by 2% NiO-impregnated sample at 9 bar and 28°C. Moreover, future studies are recommended to conduct BET surface area to provide more accurate measurements of surface area. An economic feasibility study and life cycle assessment (LCA) should also be conducted to evaluate potential implementation on a larger scale.

## ACKNOWLEDGMENT

This study was supported by 2020 Activated Carbon Research Group. The authors are grateful to colleagues from Chemical Engineering Department, University of Indonesia, who provided insight and expertise that support the completion of this study.

## REFERENCES

- [1] A. Serpe et al., "2002–2022: 20 years of e-waste regulation in the European Union and the worldwide trends in legislation and innovation technologies for a circular economy," *RSC Sustain.*, pp. 1039–1083, 2024, doi: 10.1039/d4su00548a.
- [2] L. A. Salo and I. Vanany, "A simulation model of shipment planning and storage capacity for wheat material," *IOP Conf. Ser.: Mater. Sci. Eng.*, vol. 1034, no. 1, p. 012119, 2021, doi: 10.1088/1757-899x/1034/1/012119.
- [3] S. Biloe, V. Goetz, and S. Mauran, "Characterization of adsorbent composite blocks for methane storage," *Carbon*, vol. 39, no. 11, pp. 1653–1662, 2020, doi: 10.1016/s0008-6223(00)00288-8.
- [4] M. M. Sabio and F. R. Reinoso, "Role of chemical activation in the development of carbon porosity," *Colloids Surf. A Physicochem. Eng. Asp.*, vol. 241, no. 1–3, pp. 15–25, 2024, doi: 10.1016/j.colsurfa.2004.04.007.
- [5] M. Yuliusman et al., "Activated carbon preparation from durian peel wastes,"

*Recent Prog. Energy, Communities Cities*, vol. 030020, no. Sep. 2020, pp. 1–6, 2021.

[6] S. Sharifian and N. Asasian-Kolur, “Polyethylene terephthalate (PET) waste to carbon materials: Theory, methods and applications,” *J. Anal. Appl. Pyrolysis*, vol. 163, p. 105496, 2022, doi: 10.1016/j.jaap.2022.105496.

[7] T. H. Pham, “Synthesis of activated carbon from polyethylene terephthalate (PET) plastic waste and its application for removal of organic dyes from water,” *Non-Metallic Mater. Sci.*, vol. 5, no. 1, pp. 27–37, 2023, doi: 10.30564/nmms.v5i1.5663.

[8] D. Galeano-Caro et al., “Novel activated carbon from polyethylene terephthalate waste for water vapour adsorption,” *Journal of Environmental Chemical Engineering*, vol. 13, no. 2, p. 115963, 2025, doi: 10.1016/j.jece.2025.115963.

[9] A. Ghaemi, H. Mashhadimoslem, and P. Zohourian Izadpanah, “NiO and MgO/activated carbon as an efficient CO<sub>2</sub> adsorbent: Characterization, modeling, and optimization,” *Int. J. Environ. Sci. Technol.*, vol. 19, no. 2, pp. 727–746, 2021, doi: 10.1007/s13762-021-03582-x.

[10] Z. Heidarinejad et al., “Methods for preparation and activation of activated carbon: A review,” *Environ. Chem. Lett.*, vol. 18, no. 2, pp. 393–415, 2020, doi: 10.1007/s10311-019-00955-0.

[11] J. Wang, X. Yuan, S. Deng, X. Zeng, Z. Yu, S. Li, dan K. Li, “Adsorption characteristics of methane on microporous carbon prepared from bitumite: Equilibrium, thermodynamics and site energy distribution studies,” *J. Ind. Eng. Chem.*, vol. 148, pp. 701–723, 2025, doi: 10.1016/j.jiec.2025.01.028.

[12] M. Olam, “Production of activated carbon from waste PET chars,” *Int. J. Environ. Monit. Anal.*, vol. 10, no. 2, p. 39, 2022, doi: 10.11648/j.ijema.20221002.13.

[13] R. R. Solís et al., , “Transforming a mixture of real post-consumer plastic waste into activated carbon for biogas upgrading,” *Process Saf. Environ. Prot.*, vol. 190, pp. 298–315, 2024, doi: 10.1016/j.psep.2024.07.022.

[14] Z. Zhu and M. Zhang, “Experimental studies of methane adsorption on activated carbon and 3D graphene materials,” *Processes*, vol. 11, no. 8, p. 2487, 2023, doi: 10.3390/pr11082487.

[15] S. E. Dissanayake, M. Fernando, and R. Bandara, “Sustainable valorization of PET plastic waste into porous carbon for gas adsorption and energy storage,” *Sustainable Materials and Technologies*, vol. 38, p. e00584, 2024, doi: 10.1016/j.susmat.2024. e00584

[16] Boules et al., “Turning plastic and biomass waste into adsorbents: CO<sub>2</sub>/CH<sub>4</sub> separation and comparison with commercial carbons,” *Waste Management*, vol. 210, p. 115223, 2025, doi: 10.1016/j.wasman.2025.115223

[17] M. M. Sabio and F. R. Reinoso, “Role of chemical activation in the development of carbon porosity,” *Colloids Surf. A Physicochem. Eng. Asp.*, vol. 241, no. 1–3, pp. 15–25, 2024, doi: 10.1016/j.colsurfa.2004.04.007.

[18] R. Martín-Lara et al., “Turning plastic and biomass waste into adsorbents for biogas upgrading,” *Waste Management*, vol. 210, p. 115224, 2025.

[19] J. Wang, X. Yuan, S. Deng, X. Zeng, Z. Yu, S. Li, dan K. Li, “Waste polyethylene terephthalate plastics-derived activated carbons for CO<sub>2</sub> adsorption,” *Green Chemistry*, vol. 22, no. 21, pp. 7448–7460, 2020.

[20] L. A. Salo and I. Vanany, “A simulation model of shipment planning and storage capacity for wheat material,” *IOP Conf. Ser.: Mater. Sci. Eng.*, vol. 1034, no. 1, p. 012119, 2021, doi: 10.1088/1757-899x/1034/1/012119.

[21] S. Sharifian and N. Asasian-Kolur, “Polyethylene terephthalate (PET) waste to carbon materials: Theory, methods and applications,” *J. Anal. Appl. Pyrolysis*, vol. 163, p. 105496, 2022, doi: 10.1016/j.jaap.2022.105496.

[22] Y. Wang, J. Pan, Y. Li, P. Zhang, M. Li, H. Zheng, X. Zhang, H. Li, dan Q. Du, “Methylene blue adsorption by activated carbon, nickel alginate/activated carbon aerogel, and nickel alginate/graphene oxide aerogel: A comparison study,” *J. Mater. Res. Technol.*, vol. 9, no. 6, pp. 12443–12460, 2020, doi: 10.1016/j.jmrt.2020.08.080.

[23] Z. Zhu and M. Zhang, “Experimental studies of methane adsorption on activated carbon and 3D graphene materials,” *Processes*, vol. 11, no. 8, p. 2487, 2023, doi: 10.3390/pr11082487

[24] H. T. Nguyen et al., “Activated carbon materials derived from PET plastic waste: Adsorption of organic dyes and heavy metals,” *Journal of Analytical and Applied Pyrolysis*, vol. 170, p. 106000, 2024.